



# Organic carbon dot coating for superhydrophobic aluminum alloy surfaces

Huaqiao Peng , Lin Li, Qiang Wang, Yabo Zhang, Tianming Wang, Baozhan Zheng, Hong Zhou

Received: 18 October 2020 / Revised: 21 November 2020 / Accepted: 30 November 2020  
© American Coatings Association 2021

**Abstract** A novel fluorine-free and silicon-free superhydrophobic aluminum alloy (treated-Al) is fabricated by chemical etching using hydrochloric acid and hydrogen peroxide and modified with an organic carbon dot (OCD) coating. The water contact angle (CA) of the treated-Al surface increases with the OCD concentration. When etched aluminum (etched-Al) is modified with 0.5 mg/ml OCDs, a CA of 161.4° is achieved, which indicates good nonwettability. SEM results verify that porous microstructures with cavities are uniformly distributed on the surface of etched-Al, in contrast to the bare aluminum alloy, which forms a primary rough structure. After treatment with 0.5 mg/ml OCDs, a nanoparticle coating is dispersed on the rough structures of treated-Al-0.5, which can trap air and make a water droplet essentially rest on a layer of air. The treated-Al-0.5 material has good self-cleaning properties and can sweep away contaminants at both 20 and 0°C. The Ecorr and Icorr of treated-Al-0.5 are -0.56 V and  $2.82 \times 10^{-6}$  A/cm<sup>2</sup>, respectively, which shows good anticorrosion performance.

**Keywords** Organic carbon dots, Chemical etching, Superhydrophobicity, Anticorrosion, Aluminum alloy, Self-cleaning

## Introduction

Aluminum alloys with low density, high specific strength, and excellent thermal and electrical conductivity are very important engineering materials and are widely used in automobiles, buildings, aircraft, and so on. To further widen the applications, it is necessary to create new functions for aluminum alloys. Recently, a great deal of attention has been focused on the fabrication of superhydrophobic surfaces due to their potential applications as self-cleaning,<sup>1</sup> antiicing,<sup>2</sup> and anticorrosion<sup>3</sup> materials in recent decades. In addition, surface modification is a constructive method that has the potential to create superhydrophobic surfaces and is capable of combating the transmission and spread of COVID-19 due to the self-cleaning performance of superhydrophobic surfaces.<sup>4</sup>

By mimicking the lotus effect, the common way to produce superhydrophobic surfaces usually includes two key procedures, namely rough structure creation and subsequent modification by low-surface-energy materials. Thus, various techniques have been investigated to prepare superhydrophobic surfaces, including chemical etching,<sup>5,6</sup> laser processing,<sup>7,8</sup> layer-by-layer assembly,<sup>9,10</sup> the sol-gel method,<sup>11,12</sup> chemical vapor deposition,<sup>13,14</sup> and plasma processing.<sup>15,16</sup> Although these reported fabrication methods of superhydrophobic surfaces show excellent performance, toxic low-surface-energy materials are always used, such as fluorine-containing compounds.<sup>17–19</sup> In addition, ZnO, TiO<sub>2</sub>, and SiO<sub>2</sub> are widely used during the creation of the rough structure, which may threaten human health.<sup>20–22</sup>

Therefore, eco-friendly materials are highly desired to fabricate superhydrophobic surfaces. Recently, as a new carbon nanomaterial, carbon dots (CDs) have attracted considerable attention owing to their nanometer size, good biocompatibility, low toxicity, excellent optical properties, and high photostabil-

---

H. Peng (✉), L. Li, Q. Wang, Y. Zhang,  
T. Wang, H. Zhou (✉)  
The Second Research Institute of Civil Aviation  
Administration of China, Chengdu 610041, China  
e-mail: penghuaqiao@fcc.org.cn

H. Zhou  
e-mail: zhouhong@caacsri.com

B. Zheng  
Sichuan University, Chengdu 610041, China

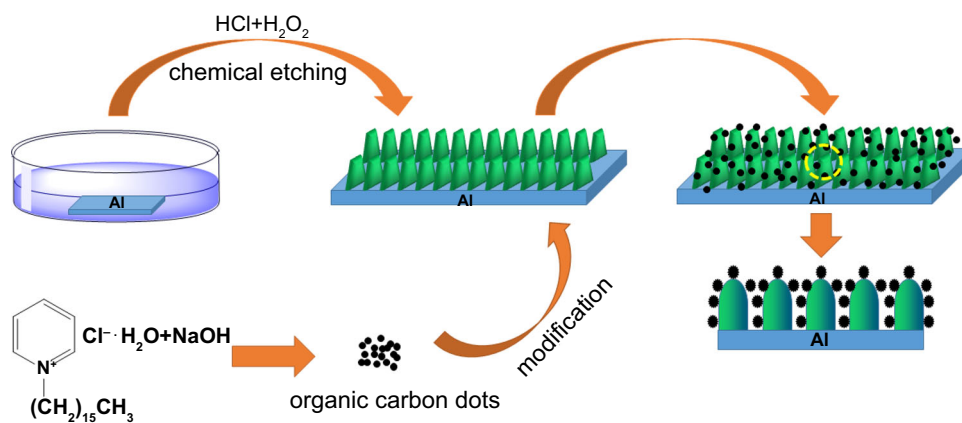


Fig. 1: Schematic diagram of the main fabrication steps of the superhydrophobic aluminum alloy surface

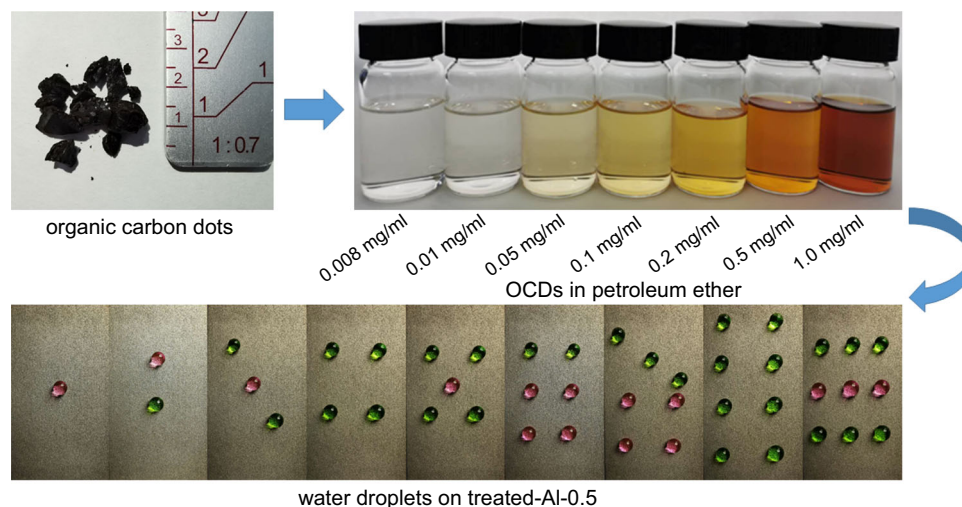


Fig. 2: Photos of OCDs, OCDs in petroleum ether, and water droplets on treated-Al-0.5 with OCD coating

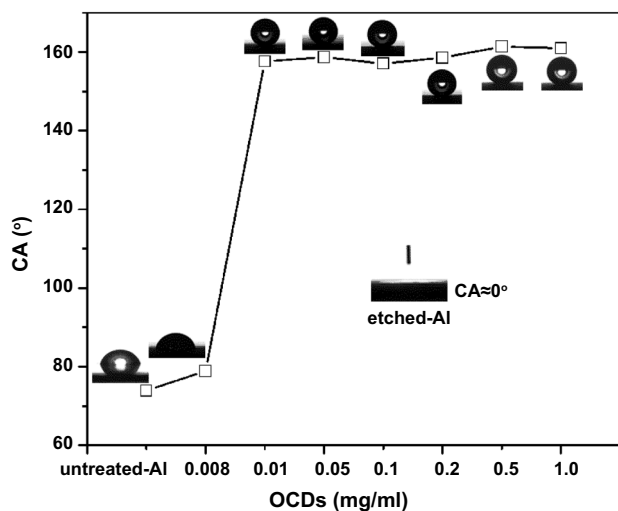


Fig. 3: CAs of aluminum alloy surfaces treated with various concentrations of OCDs

ity.<sup>23–27</sup> Considering these advantages, CDs have led to a range of potential applications, such as sensors,<sup>28</sup> solar cells,<sup>29</sup> bioimaging,<sup>30</sup> and catalysts.<sup>31</sup>

With regard to the preparation of superhydrophobic surfaces, there is no available example in the literature reporting the incorporation of CDs. In this article, we report the preparation of a novel fluorine-free and silicon-free superhydrophobic aluminum alloy surface through a facile and efficient method of chemical etching using hydrochloric acid and hydrogen peroxide at lower concentrations. The fabrication process is followed by treatment with an organic carbon dot (OCD) coating, which acts not only as the rough structure component but also the low-surface-energy modifier. The achieved superhydrophobic aluminum surface with OCD coating is characterized and evaluated in detail in terms of its wettability, self-cleaning, and anticorrosion performances.

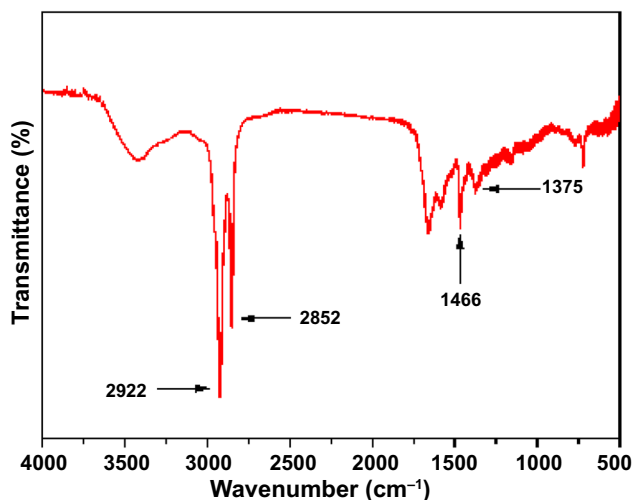


Fig. 4: FTIR spectrum of OCDs

## Experimental section

### Materials

Aluminum alloy (SAE AMS 4037) was provided by Kaiser Aluminum Corporation and cut into 50 mm × 25 mm × 2 mm pieces. Hydrochloric acid (37%, w/w), hydrogen peroxide (30%, w/w), petroleum ether (60–90°C), dichloromethane, ethanol, and acetone were supplied by Chengdu Kelong Chemical Company. Cetylpyridinium chloride monohydrate (CPC) was obtained from Sigma-Aldrich. NaOH was obtained from Guangdong Chemical Reagent Engineering-Technological Research and Development Center.

### Preparation of OCDs

NaOH (2.0 M) was added to a CPC aqueous solution (15 mM) at room temperature. The reaction could be terminated any time by adjusting the pH of the solution to neutral with HCl. After the reaction, OCDs were separated by adding CH<sub>2</sub>Cl<sub>2</sub> to extract the OCDs into the bottom organic layer. Dialysis was applied to remove the excess reagents and other water-soluble components. The OCD samples were vacuum-dried at 45°C.<sup>32</sup>

### Preparation of superhydrophobic surfaces

An SAE AMS 4037 plate was polished with sandpaper, cleaned ultrasonically in deionized water, acetone, and ethanol (each for 10 min), and dried under vacuum to produce untreated-Al. Then, the plate was etched for 15 min with a mixture of HCl (1 mol/l) and H<sub>2</sub>O<sub>2</sub> (1 mol/l). The etched plate (etched-Al) was cleaned ultrasonically in deionized water, immersed in hot water (50°C) for 1 h, rinsed with deionized water, and

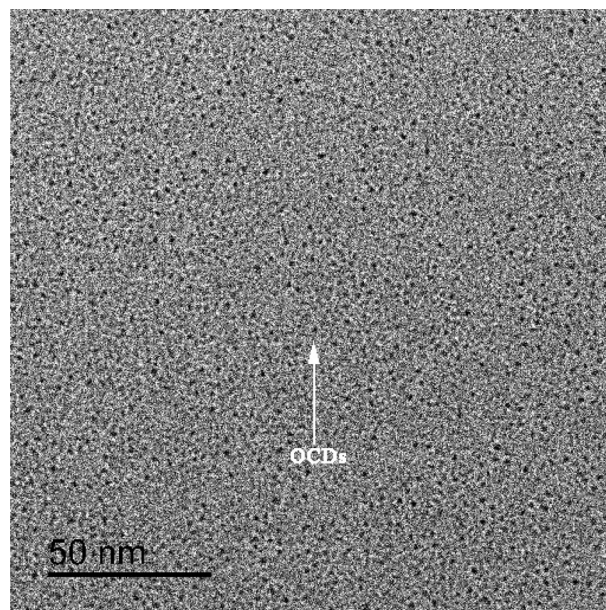


Fig. 5: TEM image of OCDs

then dried in vacuum. The OCDs were dissolved in petroleum ether at room temperature to obtain homogeneous solutions of 0.008, 0.01, 0.05, 0.1, 0.2, 0.5, and 1.0 mg/ml. The etched-Al was immersed into the solutions for 3 h to produce treated-Al-0.008, treated-Al-0.01, treated-Al-0.05, treated-Al-0.1, treated-Al-0.2, treated-Al-0.5, and treated-Al-1.0, respectively. Then, the plates (treated-Al) were dried at room temperature. The main steps of fabricating coatings on the superhydrophobic aluminum alloy surfaces are shown in Fig. 1.

### Characterization of superhydrophobic surfaces

The water contact angle (CA) was measured on a Kruss DSA30S contact angle system with a 3 μl droplet. The root-mean-square roughness (R<sub>q</sub>) of the surfaces was measured by laser scanning confocal microscopy (LSM 800, Zeiss, Germany) according to the requirements of ISO 25178. The surface roughness of each sample was measured in a 500 × 500 μm<sup>2</sup> planar area for at least three different positions. FTIR spectra were recorded in the range of 400–4000 cm<sup>-1</sup> on a Spectrum Two spectrometer (PerkinElmer, USA). Transmission electron microscopy (TEM) images were acquired on a Tecnai G2 F20 S-TWIN transmission electron microscope (FEI, USA). SEM analysis was performed with a JEOL JSM-6480A microscope. XPS data were collected on an Axis Ultra X-ray photoelectron spectrometer (XSAM 800, Kratos, UK) using a mono-Al K $\alpha$  X-ray excitation source. The anticorrosion analysis was performed in 3.5 wt% NaCl at ambient temperature via an electrochemical workstation (PARSTAT 4000A, Princeton). The Pt electrode was the counter electrode, the Ag/AgCl

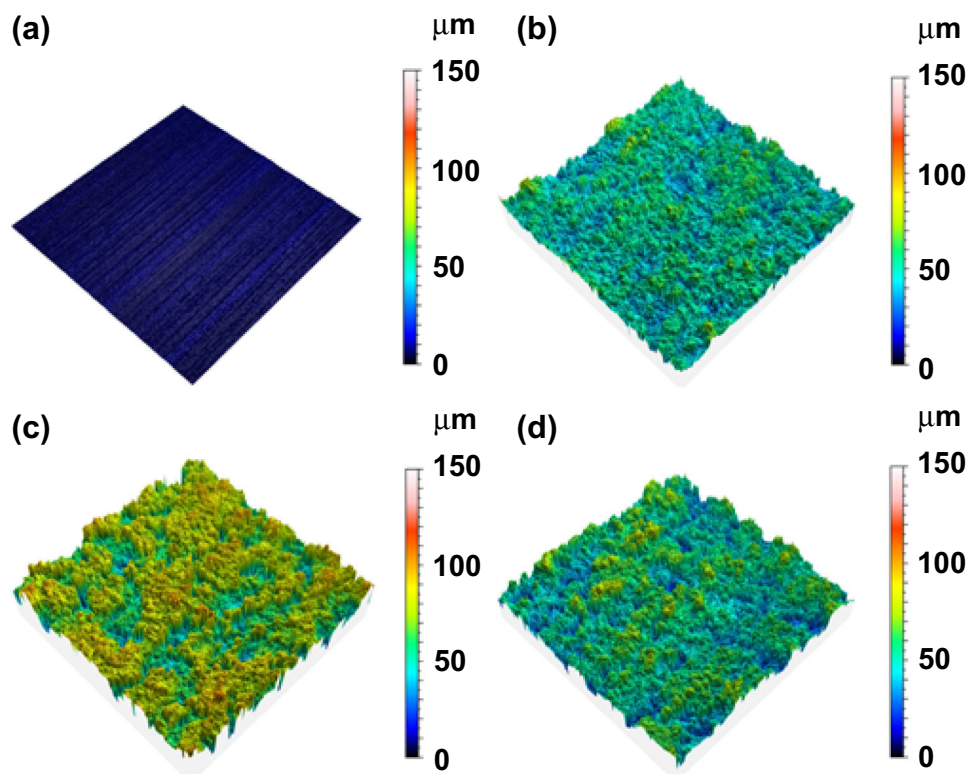


Fig. 6: LSM images of (a) untreated-Al, (b) etched-Al, (c) treated-Al-0.008, and (d) treated-Al-0.5

electrode was the reference electrode, and the samples served as the working electrode. Before testing, all the samples were immersed in the NaCl solution for 20 min to ensure the system was stabilized, and the corresponding scan rate was 1.0 mV/s.

## Results and discussion

### Wettability of aluminum surface treated with OCDs

The OCDs appear deep brown and granular and can be stably suspended in common organic solvents. Photos of different concentrations of OCDs in petroleum ether and water droplets on treated-Al-0.5 are shown in Fig. 2. Water droplets with good spherical shapes ride on the surfaces, indicating good hydrophobic properties.

From Fig. 3, it can be seen that the pristine aluminum is hydrophilic and has a CA of 73.9°. When a water droplet touches the surface of etched-Al, the water droplet slowly spreads on the surface and wets the whole surface, which makes it difficult to measure the CA value. At this time, the CA value is nearly 0°, which indicates the superhydrophilic performance of etched-Al. According to the Wenzel theory,<sup>33</sup> the hydrophilicity will be increased for a hydrophilic surface with further increasing surface roughness,

which could be explained by the above phenomenon of the more hydrophilic nature of etch-Al due to its larger roughness than that of pristine aluminum.<sup>34</sup>

The CA increases gently to 78.9° after treatment with 0.008 mg/ml OCDs. However, after treatment with 0.01 mg/ml OCDs, CA drastically increases to 157.6°. With increasing OCD concentration, CA increases accordingly, which indicates enhanced non-wettability. Furthermore, the maximum CA (161.4°) is achieved when Al is treated with 0.5 mg/ml OCDs. However, CA is not obviously increased when the OCD concentration is further increased.

Based on the equation of Cassie and Baxter,<sup>35</sup>

$$\cos \theta_c = f_1 \cos \theta - f_2 \tag{1}$$

$$f_1 + f_2 = 1 \tag{2}$$

where  $\theta_c$  and  $\theta$  are the apparent contact angles of the water droplets on the rough surface and flat surface, respectively, and  $f_1$  and  $f_2$  are the area fractions of the aluminum surface and air on the surface, respectively. In the case of the present fabricated superhydrophobic surface of treated-Al-0.5,  $\theta_c$  and  $\theta$  are 161.4° and 73.9°, respectively. It can be calculated that  $f_1$  and  $f_2$  are 0.041 and 0.959, respectively, which indicates that only approximately 4.1% of the water surface is in contact with the aluminum surface and the remaining 95.9% of the water droplet is suspended on the air. It is obvious

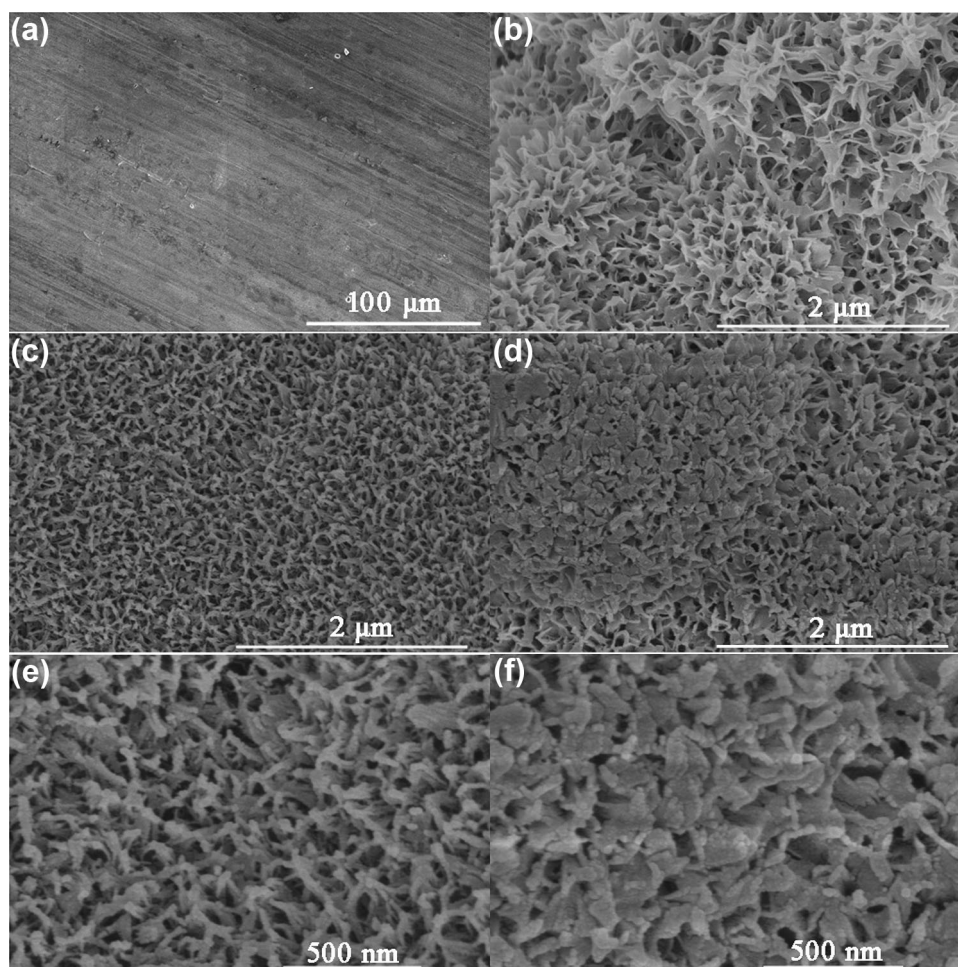


Fig. 7: SEM images of (a) untreated-Al, (b) etched-Al, (c and e) treated-Al-0.008, and (d and f) treated-Al-0.5

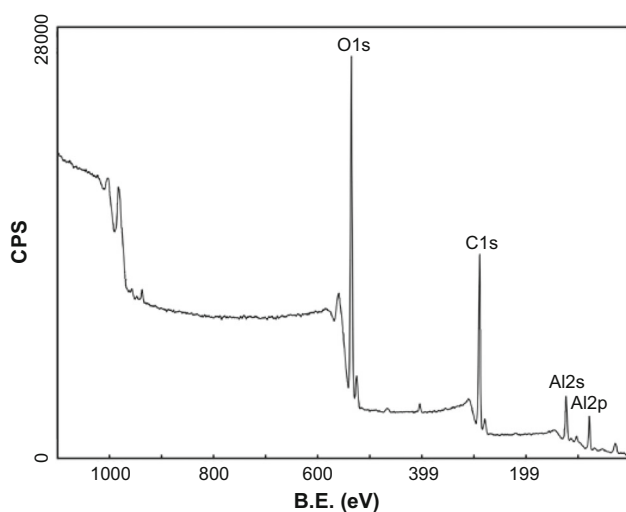


Fig. 8: XPS spectrum of treated-Al-0.5

that the contact area between the air and the water surface accounts for the overwhelming majority of the contact area. As a result, the treated-Al-0.5 exhibits good superhydrophobicity.

Figure 4 shows the FTIR spectrum of the OCDs. The observed peaks at 2922 and 2852  $\text{cm}^{-1}$  are assigned to the stretching vibration of C–H, corresponding to  $\text{CH}_3$  and  $\text{CH}_2$  moieties in CPC, respectively. The bands near 1466 and 1375  $\text{cm}^{-1}$  are attributed to  $\text{CH}_2$  stretching vibration deformation. It is believed that the concentration of OCDs has a key effect on the wettability of the as-prepared surfaces. The presence of  $\text{CH}_3$  and  $\text{CH}_2$  on OCDs is confirmed to contribute to the hydrophobic performance of treated-Al.

Figure 5 displays a TEM image of the OCDs. It is confirmed that the OCDs are spherical in shape and are well dispersed from each other. The average size of the OCDs is approximately 2 nm, which causes the OCDs to be stably suspended in petroleum ether.

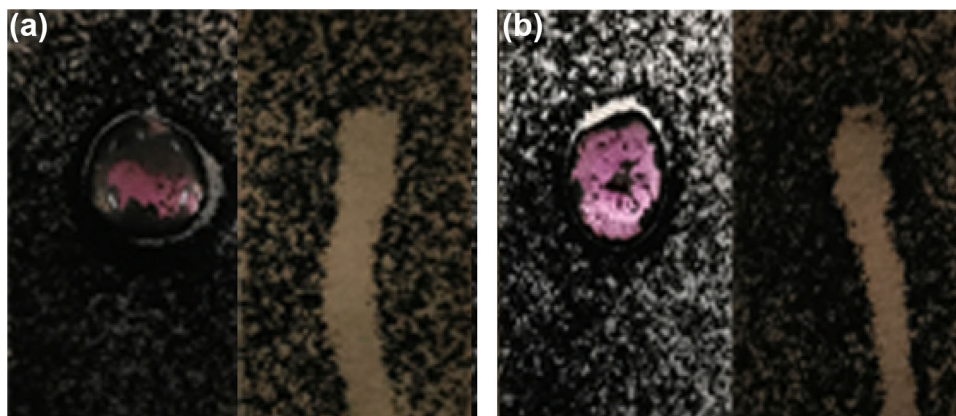


Fig. 9: Self-cleaning ability at 20°C (left: untreated-Al, right: treated-Al-0.5) (a); Self-cleaning ability at 0°C (left: untreated-Al, right: treated-Al-0.5) (b)

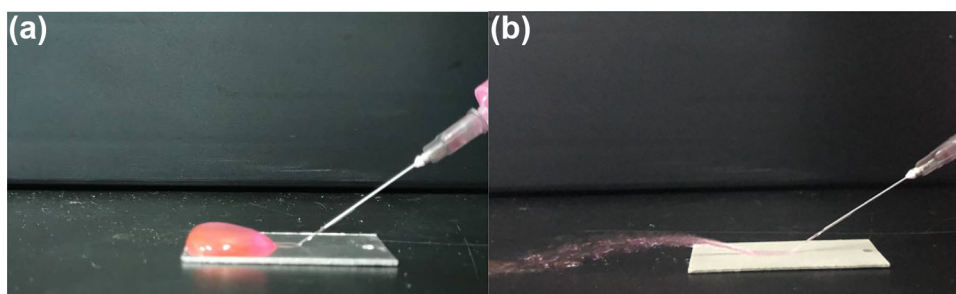


Fig. 10: Optical images of water jet impact on (a) untreated-Al and (b) treated-Al-0.5

#### *Surface morphology of aluminum surface treated with OCDs*

To understand the surface structure, the morphology and roughness of the as-prepared superhydrophobic surface were studied from LSM images. From Fig. 6, it is observed that the surfaces exhibit different rough surface structures. The surface roughness  $R_q$  of untreated-Al is only 0.654  $\mu\text{m}$ , which is flat and smooth. As shown in the LSM data,  $R_q$  increases to 8.24  $\mu\text{m}$  when aluminum is chemically etched with HCl and  $\text{H}_2\text{O}_2$ , which indicates the improved roughness on the surface. After the etched-Al was modified with OCDs, the continuous uniformity distribution of OCDs on the Al alloy surface was verified, and  $R_q$  was further increased. For treated-Al-0.008 and treated-Al-0.5, the  $R_q$  values are 15.8  $\mu\text{m}$  and 12.2  $\mu\text{m}$ , respectively. This enables the formation of superhydrophobic surfaces with micro/nanoscale surface roughness. Although the roughness of treated-Al-0.5 is less than that of treated-Al-0.008, the CA of treated-Al-0.5 is much larger. It is proposed that the proper roughness is a key factor in acquiring a superhydrophobic surface, which does not mean that a larger roughness is better.

The micromorphology of the untreated-Al and treated-Al surfaces was further researched by SEM.

From Fig. 7a, the Al surface is relatively flat. It is observed that all the treated-Al surfaces exhibit different hydrangea-like rough surface structures. For etched-Al, the microscale pores and nanoscale flakes form a hierarchical structure on the surface. Nanosized OCDs are deposited on top of this rough surface in the form of physical adsorption and cannot be washed away easily. After treatment with 0.008 mg/ml OCDs, the surface is randomly dotted with many microscale spherical clusters with an average diameter of approximately 60 nm (Fig. 7e), indicating that the surface has a hierarchical micro-nanostructure with a CA of 78.9°. After treatment with 0.5 mg/ml OCDs, while innumerable nanopores orthogonally align with local facets on the Al surface, under larger magnification, it can be seen that the granulates are distributed on these rough structures (Fig. 7f), which enables Al to acquire good water repellence with a CA of 161.4°. Due to the absorption and van der Waals interactions on the surface, the low-surface-energy materials combine with a unique hierarchical structure introduced by the nanosize OCDs, providing sufficient roughness to stably trap a great deal of air to decrease the contact area between the water droplet and the solid surface, enhancing the superhydrophobicity, which corresponds to the Cassie state.<sup>35</sup>

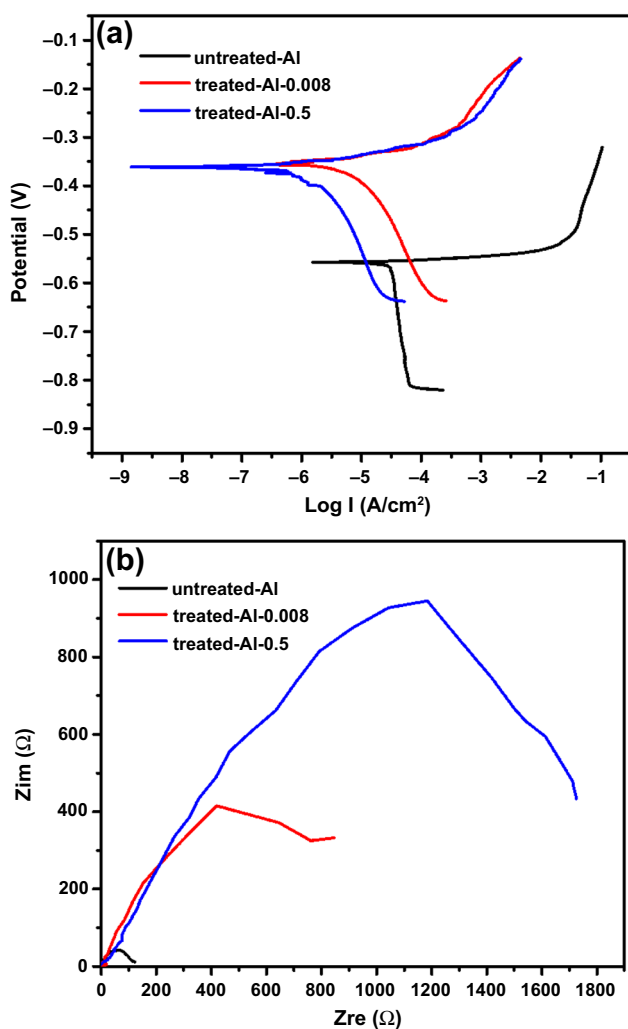


Fig. 11: Tafel curves of untreated-Al and treated-Al (a); EIS results for untreated-Al and treated-Al (b)

### Surface composition

XPS was performed to investigate the surface chemistry of the samples. From the full survey spectrum (Fig. 8), signals of C 1s, O 1s, Al 2s and Al 2p peaks are all detected. Two main signal peaks, corresponding to carbon (C 1s, 284.8 eV) and oxygen (O 1s, 531.2 eV), appear in the spectrum. From the XPS study, it is evident that the chemical composition of the aluminum surface remains unaltered. Furthermore, we can infer that a low-surface-energy coating of OCDs is formed on the aluminum substrates. Based on the above analyses, it can be concluded that the combination of hierarchical structure and chemical composition is very important to construct a superhydrophobic surface.

### Self-cleaning and anticorrosion applications

The corresponding self-cleaning properties were determined using black charcoal powder as an artificial contaminant at temperatures of 20 and 0°C. As shown in Fig. 9, it was clearly observed that water droplets pick up contaminants and slide away from the surface of treated-Al-0.5 at a temperature of 20°C. Moreover, the good self-cleaning properties of treated-Al-0.5 are not obviously influenced by the lower temperature, the contaminants can be washed away by the water droplets, and no residue on the trail is left at 0°C. It was confirmed that this hierarchical superhydrophobic surface has excellent self-cleaning properties. The impact of a high-speed jet of water on the surface of untreated-Al and treated-Al-0.5 was also investigated. From Fig. 10, it can be seen that the reflected water jet can be easily bounced off and prevents water droplets from accumulating on the surface of treated-Al-0.5, which also confirms the mechanical stability of the

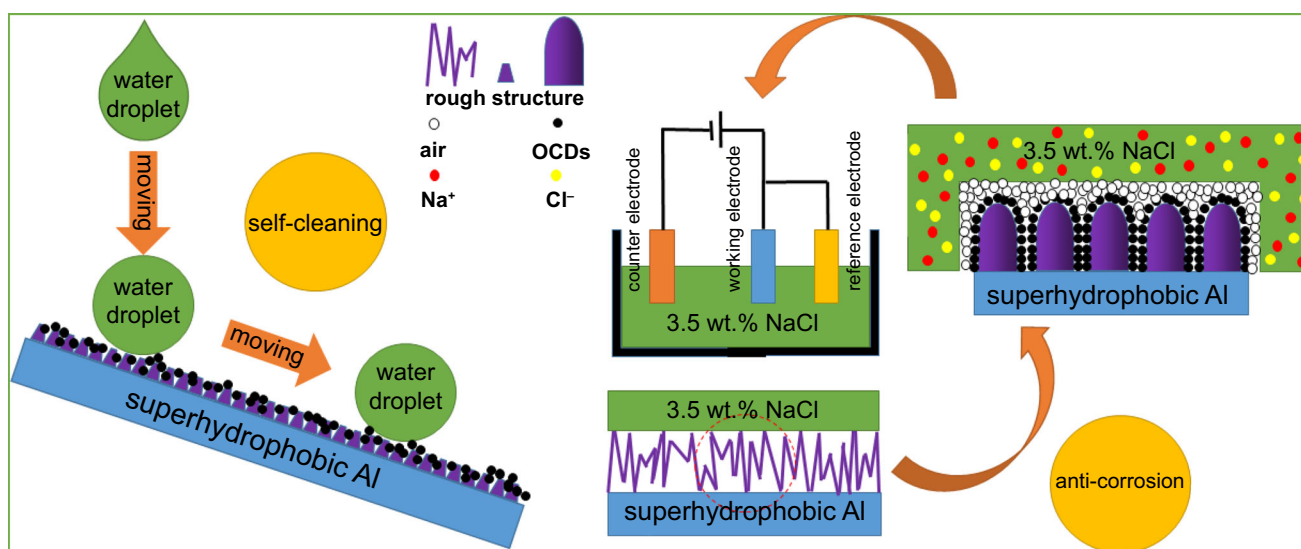


Fig. 12: Schematic illustration of water droplets in contact with the superhydrophobic aluminum alloy surface

superhydrophobicity. This is attributed to the strong physical adsorption of OCDs in the hierarchical micro-nanostructure. However, on the surface of untreated-Al, the bouncing phenomenon is not observed, and the water spreads and accumulates.

From Fig. 11a, it can be seen that the corrosion potential ( $E_{\text{corr}}$ ) of untreated-Al is  $-0.56$  V, which is the lowest among the test results. Compared to untreated-Al, the  $E_{\text{corr}}$  of treated-Al-0.5 is positively shifted and increased to  $-0.35$  V. Moreover, the corrosion current density ( $I_{\text{corr}}$ ) of treated-Al-0.5 is decreased to  $2.82 \times 10^{-6}$  A/cm<sup>2</sup>, which is the lowest. Generally, a surface with a positively shifted  $E_{\text{corr}}$  and a low corrosion current density  $I_{\text{corr}}$  can lead to superior corrosion resistance.<sup>36</sup> It is obvious that the untreated-Al substrate exhibits the worst anticorrosion performance among these samples. This is a result of the reactive chlorine ions abundant in the liquid (3.5 wt% NaCl aqueous solution), which can corrode Al substrates and lead to penetrating and pitting failures. However, the anticorrosion properties of the Al alloy were greatly enhanced after modification by chemical etching and OCD coating. Moreover, the superhydrophobic surface of treated-Al-0.5 has the best anticorrosion performance compared with the other two samples.

The corrosion resistance of the superhydrophobic surface was further explored by EIS. As shown in Fig. 11b, treated-Al has a higher impedance value than untreated-Al. In general, the larger the radius is, the better the corrosion resistance of the material. The results show that the anticorrosion performance of treated-Al is much better than that of untreated-Al.

The self-cleaning and corrosion resistance performance mechanisms could probably be related to the hydrophobicity of the Al surface (see Fig. 12). During self-cleaning, the air trapped in the space around the hierarchical structure of treated-Al-0.5 could reduce the contact area between the water droplet and the superhydrophobic surface so that the water droplet can easily slip from the superhydrophobic surface and wash away contaminants. With regard to the anticorrosion properties, the entrapped air in the interface between the solid (treated-Al) and liquid (3.5 wt% NaCl aqueous solution) can interfere with the penetration of water into the substrate. Hence, electron transfer is blocked, which leads to a lower corrosion speed and keeps corrosive media away from the surface to provide better corrosion protection. This result indicates that the superhydrophobic surface is effective for improving the corrosion resistance of aluminum.

## Conclusions

Superhydrophobic surfaces have been fabricated in this work by combining chemical etching and organic carbon dots (OCDs). Coating with OCDs at a concentration of 0.01 mg/ml or above helps to form a

continuous hierarchical micro-nanostructure on the surface of etched-Al. Then, the resulting treated-Al shows good hydrophobic behavior, and the self-cleaning and corrosion resistance of the plate is improved. The results provide a new approach to prepare superhydrophobic surfaces of materials through a low-cost and environmentally friendly OCD coating, in addition to the traditional modification of fluorine or silicon.

**Acknowledgments** This work is financially supported by the National Natural Science Foundation of China (U1833202).

**Conflict of interest** There are no conflicts of interest to declare.

## References

- Huang, YF, Chen, B, Lv, ZS, Guo, F, “Facile Fabrication of Durable Superhydrophobic SiO<sub>2</sub>/Polyacrylate Composite Coatings with Low Nanoparticle Filling.” *J. Coat. Technol. Res.*, **17** 1289–1295 (2020)
- Tong, W, Xiong, DS, Wang, N, Wu, Z, Zhou, HJ, “Mechanically Robust Superhydrophobic Coating for Aeronautical Composite Against Ice Accretion and Ice Adhesion.” *Compos. Part B Eng.*, **176** 107267 (2019)
- Arulkalam, IO, Li, Y, “Anticorrosion and Barrier Properties Appraisal of Poly(dimethylsiloxane)-ZnO Nanocoating Transition from Superhydrophobic to Hydrophobic State.” *J. Coat. Technol. Res.*, **16** 1077–1088 (2019)
- Meguid, SA, Elzaabalawy, A, “Potential of Combating Transmission of COVID-19 Using Novel Self-Cleaning Superhydrophobic Surfaces: Part I—Protection Strategies Against Fomites.” *Int. J. Mech. Mater. Des.*, **16** 423–431 (2020)
- Huang, Y, Sarkar, DK, Chen, XG, “Superhydrophobic Aluminum Alloy Surfaces Prepared by Chemical Etching Process and Their Corrosion Resistance Properties.” *Appl. Surf. Sci.*, **356** 1012–1024 (2015)
- Xue, CH, Li, YR, Zhang, P, Ma, JZ, Jia, ST, “Washable and Wear-Resistant Superhydrophobic Surfaces with Self-Cleaning Property by Chemical Etching of Fibers and Hydrophobization.” *ACS Appl. Mater. Interf.*, **6** 10153–10161 (2014)
- Liang, LS, Lu, LS, Xing, D, Wan, ZP, Tang, Y, “Preparation of Superhydrophobic and Anti-Resin-Adhesive Surfaces with Micro/nanoscale Structures on High-Speed Steel via Laser Processing.” *Surf. Coat. Tech.*, **357** 57–68 (2019)
- Li, J, Zhao, SC, Du, F, Zhou, YL, Yu, HD, “One-step Fabrication of Superhydrophobic Surfaces with Different Adhesion via Laser Processing.” *J. Alloy. Compd.*, **739** 489–498 (2018)
- Zheng, LZ, Su, XJ, Lai, XJ, Chen, WJ, Li, HQ, Zeng, XR, “Conductive Superhydrophobic Cotton Fabrics via Layer-by-Layer Assembly of Carbon Nanotubes for Oil-Water Separation and Human Motion Detection.” *Mater. Lett.*, **253** 230–233 (2019)
- Yang, J, Li, H, Lan, TQ, Peng, LC, Cui, RQ, Yang, H, “Preparation, Characterization, and Properties of Fluorine-



- Free Superhydrophobic Paper Based on Layer-by-Layer Assembly.” *Carbohydr. Polym.*, **178** 228–237 (2017)
11. Wu, X, Fu, Q, Kumar, D, Ho, JWC, Kanhere, P, Zhou, H, Chen, Z, “Mechanically Robust Superhydrophobic and Superoleophobic Coatings Derived by Sol–Gel Method.” *Mater. Design.*, **89** 1302–1309 (2016)
  12. Su, XJ, Li, HQ, Lai, XJ, Zhang, L, Wang, J, Liao, XF, Zeng, XR, “Vapor-Liquid Sol–Gel Approach to Fabricating Highly Durable and Robust Superhydrophobic Polydimethylsiloxane Silica Surface on Polyester Textile for Oil–Water Separation.” *ACS Appl. Mater. Interf.*, **9** 28089–28099 (2017)
  13. Sun, W, Wang, LD, Yang, ZQ, Li, SJ, Wu, TT, Liu, GC, “Fabrication of Polydimethylsiloxane-Derived Superhydrophobic Surface on Aluminium via Chemical Vapour Deposition Technique for Corrosion Protection.” *Corros. Sci.*, **128** 176–185 (2017)
  14. Khan, AF, Huang, K, Hu, M, Yu, XG, Yang, DR, “Wetting Behavior of Metal-Catalyzed Chemical Vapor Deposition-Grown One-Dimensional Cubic-SiC Nanostructures.” *Langmuir*, **34** 5214–5224 (2018)
  15. Castaneda-Montes, I, Ritchie, AW, Badyal, JPS, “Atomised Spray Plasma Deposition of Hierarchical Superhydrophobic Nanocomposite Surfaces.” *Colloids Surf. A*, **558** 192–199 (2018)
  16. Liu, S, Zhou, H, Wang, HX, Zhao, Y, Shao, H, Xu, ZG, Feng, ZH, Liu, DQ, Lin, T, “Argon Plasma Treatment of Fluorine-Free Silane Coatings: A Facile, Environment-Friendly Method to Prepare Durable, Superhydrophobic Fabrics.” *Adv. Mater. Interf.*, **4** 1700027 (2017)
  17. Wang, HX, Zhuang, J, Qi, HY, Yu, JT, Guo, ZJ, Ma, YH, “Laser-Chemical Treated Superhydrophobic Surface as a Barrier to Marine Atmospheric Corrosion.” *Surf. Coat. Technol.*, **401** 126255 (2020)
  18. Vanithakumari, SC, Jena, G, Sofia, S, Thinaharan, C, George, RP, Philip, J, “Fabrication of Superhydrophobic Titanium Surfaces with Superior Antibacterial Properties Using Graphene Oxide and Silanized Silica Nanoparticles.” *Surf. Coat. Technol.*, **400** 126074 (2020)
  19. Sun, RY, Zhao, J, Li, Z, Qin, N, Mo, JL, Pan, YJ, Luo, DB, “Robust Superhydrophobic Aluminum Alloy Surfaces with Anti-Icing Ability, Thermostability, and Mechanical Durability.” *Prog. Org. Coat.*, **147** 105745 (2020)
  20. Zhang, X, Si, YF, Mo, JL, Guo, ZG, “Robust Micro-nanoscale Flowerlike ZnO/Epoxy Resin Superhydrophobic Coating with Rapid Healing Ability.” *Chem. Eng. J.*, **313** 1152–1159 (2017)
  21. Zhang, M, Xiao, YX, Lian, XW, Dong, Y, “Measuring Failure Pressure of Porous Superhydrophobic Coatings via Microfluidic Method.” *Appl. Phys. A.*, **124** 579 (2018)
  22. Zhang, XF, Zhao, JP, Hu, JM, “Abrasion-Resistant, Hot Water-Repellent and Self-Cleaning Superhydrophobic Surfaces Fabricated by Electrophoresis of Nanoparticles in Electrodeposited Sol-Gel Films.” *Adv. Mat. Interf.*, **4** 1700177 (2017)
  23. Long, P, Feng, Y, Li, Y, Cao, C, Li, S, An, H, Qin, C, Han, J, Feng, W, “Solid-State Fluorescence of Fluorine-Modified Carbon Nanodots Aggregates Triggered by Poly(Ethylene Glycol).” *ACS Appl. Mater. Interf.*, **9** 37981–37990 (2017)
  24. Pritzl, SD, Pschunder, F, Ehrat, F, Bhattacharyya, S, Lohmüller, T, Huergo, MA, Feldmann, J, “Trans-Membrane Fluorescence Enhancement by Carbon Dots: Ionic Interactions and Energy Transfer.” *Nano. Lett.*, **19** 3886–3891 (2019)
  25. Wang, YR, Li, YH, Xu, Y, “Synthesis of Mechanical Responsive Carbon Dots with Fluorescence Enhancement.” *J. Colloid. Interf. Sci.*, **560** 85–90 (2020)
  26. Kundu, A, Park, B, Oh, JY, Sankar, KV, Ray, C, Kim, WS, Jun, SC, “Multicolor Emissive Carbon Dot with Solvatochromic Behavior Across the Entire Visible Spectrum.” *Carbon*, **156** 110–118 (2020)
  27. Yap, SHK, Chan, KK, Zhang, G, Tjin, SC, Yong, KT, “Carbon Dot-Functionalized Interferometric Optical Fiber Sensor for Detection of Ferric Ions in Biological Samples.” *ACS Appl. Mater. Interf.*, **11** 28546–28553 (2019)
  28. Zhang, LL, Han, YJ, Zhu, JB, Zhai, YL, Dong, SJ, “Simple and Sensitive Fluorescent and Electrochemical Trinitrotoluene Sensors Based on Aqueous Carbon Dots.” *Anal. Chem.*, **87** 2033–2036 (2015)
  29. Matta, SK, Zhang, CM, O’Mullane, AP, Du, AJ, “Density Functional Theory Investigation of Carbon Dots as Hole-transport Material in Perovskite Solar Cells.” *Chem. Phys. Chem.*, **19** 3018–3023 (2018)
  30. Atchudan, R, Edison, TNJI, Perumal, S, Vinodh, R, Lee, YR, “In-Situ Green Synthesis of Nitrogen-Doped Carbon Dots for Bioimaging and TiO<sub>2</sub> Nanoparticles @Nitrogen-Doped Carbon Composite for Photocatalytic Degradation of Organic Pollutants.” *J. Alloy. Compd.*, **766** 12–24 (2018)
  31. Sharma, S, Mehta, SK, Ibhaddon, AO, Kansal, SK, “Fabrication of Novel Carbon Quantum Dots Modified Bismuth Oxide ( $\alpha$ -Bi<sub>2</sub>O<sub>3</sub>/C-dots): Material Properties and Catalytic Applications.” *J. Colloid. Interf. Sci.*, **533** 227–237 (2019)
  32. Zheng, BZ, Liu, T, Paa, MC, Wang, MN, Liu, Y, Liu, LZ, Wu, CF, Du, J, Xiao, D, Choi, MMF, “One Pot Selective Synthesis of Water and Organic Soluble Carbon Dots with Green Fluorescence Emission.” *RSC Adv.*, **5** 11667–11675 (2015)
  33. Wenzel, RN, “Resistance of Solid Surfaces to Wetting by Water.” *Ind. Eng. Chem.*, **28** 988–994 (1936)
  34. Wei, ZB, Jiang, DY, Chen, J, Ren, S, Li, L, “Fabrication of Mechanically Robust Superhydrophobic Aluminum Surface by Acid Etching and Stearic Acid Modification.” *J. Adhes. Sci. Technol.*, **31** 2380–2397 (2017)
  35. Cassie, ABD, Baxter, S, “Wettability of Porous Surfaces.” *Trans. Faraday Soc.*, **40** 546–551 (1944)
  36. Li, XW, Zhang, L, Shi, T, Zhang, CW, Zhang, LC, “Facile Preparation of Superhydrophobic Structures on Al Alloys Surfaces with Superior Corrosion Resistance.” *Mater. Corros.*, **70** 558–565 (2019)

**Publisher’s Note** Springer Nature remains neutral with regard to jurisdictional claims in published maps and institutional affiliations.